

Multi-objective Optimum Design of Balanced SAW Filters Using Generalized Differential Evolution

KIYOHARU TAGAWA

School of Science and Engineering

Kinki University

3-4-1 Kowakae, Higashi-Osaka, 577-8502

JAPAN

tagawa@info.kindai.ac.jp

Abstract: A multi-objective optimum design method of the balanced Surface Acoustic Wave (SAW) filter is proposed. The frequency response characteristics of the balanced SAW filters are governed primarily by their geometrical structures. Besides, specifications for a balanced SAW filter is given by using several criteria. Therefore, in order to realize desirable frequency response characteristics, the structural design of the balanced SAW filter is formulated as a constrained multi-objective optimization problem. Then a recent Evolutionary Multi-objective Optimization (EMO) algorithm, which is called Generalized Differential Evolution 3 (GED3), is applied to the multi-objective optimization problem. Furthermore, in order to clarify the tradeoff relationship among the objective functions of the multi-objective optimization problem, Principal Component Analysis (PCA) is used to assess the set of the non-dominated solutions obtained by GDE3. Finally, the proposed optimum design method is demonstrated in the three- and the two-objective optimum design problems of a practical balanced SAW filter.

Key-Words: Surface acoustic wave filter, differential evolution, multi-objective optimization

1 Introduction

Surface Acoustic Wave (SAW) filters are small, rugged and cost-competitive mechanical band-pass filters with outstanding frequency response characteristics. Therefore, SAW filters have played an important role as a key device in various mobile and wireless communication systems such as personal digital assistants (PDAs) and cellular phones[1, 2]. Recently, the balanced SAW filter becomes widely used in the modern Radio Frequency (RF) circuits of cellular phones. That is because the balanced SAW filter can provide not only the band-pass filtering function but also some external functions such as the unbalance-balance signal conversion, the impedance conversion and so on[3]. Consequently, by using the balanced SAW filter, we can reduce the total number of the components of the modern RF circuit, as well as their mounted area. As a result, we can miniaturize the modern RF circuits of cellular phones.

The frequency response characteristics of SAW filters including balanced ones are governed primarily by their geometrical structures, namely, the configurations of Inter-Digital Transducers (IDTs) and Shorted Metal Strip Arrays (SMSAs) reflectors fabricated on piezoelectric substrates. Therefore, in order to realize desirable frequency response characteristics of SAW filters, we have to decide their suitable struc-

tures, which are specified by some design parameters such as the numbers of the electrodes of IDTs.

In order to decide a suitable structure of the SAW filter, optimum design methods that combine the optimization algorithm with the computer simulation have been reported[4, 5, 6, 7]. By the way, Evolutionary Algorithms (EAs) such as Genetic Algorithm (GA) are practical optimization algorithms and applied to various optimum design problems effectively[8, 9]. Therefore, GAs have been also applied to the optimum design problem of SAW filters[10, 11]. In our previous paper[12], a recent EA called Differential Evolution (DE)[13] was applied to the optimum design problem of a practical balanced SAW filter.

Specifications for the balanced SAW filter are described by using several criteria. However, in our previous optimum design method[12], the structural design of the balanced SAW filter was formulated as a single-objective optimization problem. Exactly speaking, a single-objective function was defined by the weighted sum of the several criteria of the balanced SAW filter. One difficulty in our previous optimum design method is the choice of appropriate weighting coefficients. Therefore, even if a very good solution could be obtained for the single-objective optimization problem, we do not necessarily obtain a desirable structure of the balanced SAW filter.

In this paper, a multi-objective optimum design method for balanced SAW filters is proposed. First of all, in order to evaluate the performance of the balanced SAW filter based on the computer simulation, the network model of the balanced SAW filter is derived from the equivalent circuit model of IDT[14]. Furthermore, several criteria of the balance and the filter characteristics of the balanced SAW filter are defined. Then, by using these criteria, the structural design of the balanced SAW filter is formulated as a constrained multi-objective optimization problem.

In order to obtain various Pareto-optimal solutions for the above multi-objective optimization problem, a recent Evolutionary Multi-objective Optimization (EMO) algorithm, which is called Generalized Differential Evolution 3 (GED3)[15], is employed. GDE3 is an extension of DE[13] for global optimization with an arbitrary number of objectives and constraints over continuous space. However, the design parameters of the balanced SAW filter take not only continuous values but also discrete values. Therefore, in order to apply GED3 to the optimum design problem of the balanced SAW filter, we employ a technique that represents various design parameters by using only real-parameters[12]. Furthermore, Principal Component Analysis (PCA) is used to assess the set of the non-dominated solutions obtained by GDE3.

Finally, the proposed multi-objective optimum design method is demonstrated on the structural design of a practical balanced SAW filter. In the optimum design problem of the balanced SAW filter, three objective functions about the filter characteristics are defined respectively within three different bandwidths. Furthermore, besides the boundary constraints on the design parameters, six non-linear constraints are considered. GDE3 is applied successfully to the three-objective optimization problem. As a result of PCA, it is found that two of the three objective functions are in the tradeoff relationship but one of them is redundant. Therefore, the redundant objective is converted into a new constraint. Then GDE3 is applied again to the revised optimum design problem with two objectives and seven non-linear constraints.

2 Balanced SAW Filter

2.1 Structure and Principle

The balanced SAW filter consists of several components, namely, Inter-Digital Transducers (IDTs) and Shorted Metal Strip Array (SMSA) reflectors fabricated on a piezoelectric substrate. Figure 1 illustrates a typical structure of the balanced SAW filter that consists of nine components: one transmitter IDT (IDT-T), two receiver IDTs (IDT-Rs), pitch-

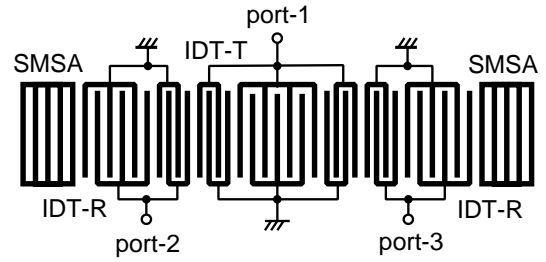


Figure 1: Balanced SAW filter

modulated IDTs between IDT-T and IDT-R, and two SMSA reflectors[16]. In the balanced SAW filter in Fig. 1, port-1 is an unbalanced input-port, while a pair of port-2 and port-3 is a balanced output-port.

2.2 Network Model of SAW Filter

In order to analyze the frequency response characteristics of balanced SAW filters based on the computer simulation, a numerical model of them is derived.

First of all, Fig. 2 illustrates two types of the configurations of IDTs with N -pair of fingers. The behavior of both types of IDTs can be analyzed by using a three-port circuit model shown in Fig. 3: port-A and port-B are acoustic-signal ports, while port-C is an electric-signal port[14]. Circuit elements included in the circuit model of IDT are given as follows.

$$\left[\begin{array}{l} A_{10} = \tanh\left(\frac{\gamma_s}{2}\right) \tanh(N\gamma_s) \\ A_{20} = \mp A_{10} \\ Z_1 = \frac{1}{R_0 F_s} \tanh(N\gamma_s) \\ Z_2 = \frac{1}{R_0 F_s} \operatorname{cosech}(2N\gamma_s) \\ Y_m = \frac{2F_s}{R_0} \tanh\left(\frac{\gamma_s}{2}\right) \\ \left[2N - \tanh\left(\frac{\gamma_s}{2}\right) \tanh(N\gamma_s) \right] \\ C_T = N C_{so} \frac{K\left(\sin\left(\eta\frac{\pi}{2}\right)\right)}{K\left(\cos\left(\eta\frac{\pi}{2}\right)\right)} \end{array} \right. \quad (1)$$

where, the dual sign (\mp) means that the minus ($-$) is for $2N$ being an even number, while the plus ($+$) is for $2N$ being an odd number. R_0 denotes characteristic impedance. F_s is image admittance and γ_s is image transfer constant. $K(z)$ is the complete elliptic integral of the first kind of a real number $z \in \mathbb{R}$.

Besides, shorting the electric port (port-C) of the equivalent circuit model of IDT in Fig. 3, the equivalent circuit model of SMSA reflector is obtained[14].

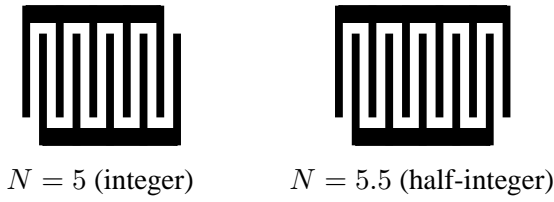


Figure 2: Configuration of N -pair of IDT

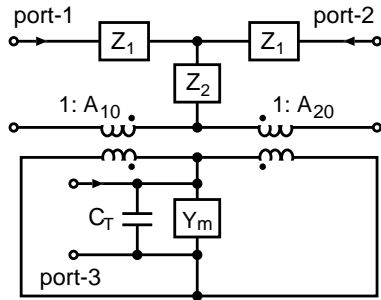


Figure 3: Equivalent circuit model of IDT

Since the components of the balanced SAW filter in Fig. 1 are connected acoustically in cascade on a piezoelectric substrate, the equivalent circuit model of the balanced SAW filter can be composed from their components' circuit models. Then the equivalent circuit model of the balanced SAW filter is represented by an admittance matrix $\mathbf{Y} = [y_{pq}]$ as follows.

$$\begin{bmatrix} I_1 \\ I_2 \\ I_3 \end{bmatrix} = \begin{bmatrix} y_{11} & y_{12} & y_{13} \\ y_{21} & y_{22} & y_{23} \\ y_{31} & y_{32} & y_{33} \end{bmatrix} \begin{bmatrix} V_1 \\ V_2 \\ V_3 \end{bmatrix} \quad (2)$$

where, V_p and I_p denote the electric current and the voltage of the port- p ($p = 1, 2, 3$) in Fig. 1.

Furthermore, considering the impedances of the input-port Z_{in} and the output-port Z_{out} , the admittance matrix \mathbf{Y} shown in (2) can be transformed into a scattering matrix $\mathbf{S} = [s_{pq}]$ as follows[12].

$$\begin{bmatrix} b_1 \\ b_2 \\ b_3 \end{bmatrix} = \begin{bmatrix} s_{11} & s_{12} & s_{13} \\ s_{21} & s_{22} & s_{23} \\ s_{31} & s_{32} & s_{33} \end{bmatrix} \begin{bmatrix} a_1 \\ a_2 \\ a_3 \end{bmatrix} \quad (3)$$

where, $\mathbf{S} = \mathbf{B} \mathbf{A}^{-1}$; \mathbf{A} and \mathbf{B} are given as follows.

$$\mathbf{A} = \begin{bmatrix} 1 + Z_{in} y_{11} & Z_{in} y_{12} & Z_{in} y_{13} \\ -Z_{out} y_{21} & 1 + Z_{out} y_{22} & -Z_{out} y_{23} \\ -Z_{out} y_{31} & -Z_{out} y_{32} & 1 + Z_{out} y_{33} \end{bmatrix}$$

$$\mathbf{B} = \begin{bmatrix} 1 - Z_{in} y_{11} & -Z_{in} y_{12} & -Z_{in} y_{13} \\ Z_{out} y_{21} & 1 + Z_{out} y_{22} & Z_{out} y_{23} \\ Z_{out} y_{31} & Z_{out} y_{32} & 1 + Z_{out} y_{33} \end{bmatrix}$$

From the scattering matrix \mathbf{S} in (3), the network model of the balanced SAW filter in Fig. 1 can be represented graphically as shown in Fig. 4. In the network model, nodes a_q ($q = 1, 2, 3$) denote the input signals of the balanced SAW filter, while nodes b_p ($p = 1, 2, 3$) denote the output signals. Scattering parameters s_{pq} labeled on edges provide the transition characteristics from input signals a_q to output signals b_p . Furthermore, a pair of port-2 and port-3 of the network model corresponds to the balanced output-port of the balanced SAW filter shown in Fig. 1, while port-1 corresponds to the unbalanced input-port.

2.3 Criteria of Balance Characteristics

In the balanced SAW filter, it is desirable that the output signals b_2 and b_3 from the balanced output-port, namely, a pair of port-2 and port-3 of the network model in Fig. 4, have the same amplitude and 180 degrees phase difference through the pass-band. In order to evaluate those balance characteristics, we employ two criteria that should be restricted to small values[4]. The amplitude balance of the balanced SAW filter is evaluated with criterion E_1 in (4). On the other hand, the phase balance of the balanced SAW filter is evaluated with criterion E_2 in (5).

$$E_1 = 20 \log_{10}(|s_{21}|) - 20 \log_{10}(|s_{31}|) \quad (4)$$

$$E_2 = \varphi(s_{21}) - \varphi(s_{31}) + 180 \quad (5)$$

where, $\varphi(s_{pq})$ denotes the phase angle of s_{pq} .

2.4 Criteria of Filter Characteristics

In order to evaluate the band-pass filter characteristics of the balanced SAW filter strictly, we have to segregate the differential mode signal from the common mode signal in the network model in Fig. 4. Therefore, according to the balanced network theory[17], the differential mode signals a_d and b_d are derived from a_q ($q = 2, 3$) and b_p ($p = 2, 3$) as shown in (6). Similarly, the common mode signals a_c and b_c are also derived from them as shown in (7).

$$\begin{cases} a_d = \frac{1}{\sqrt{2}}(a_2 - a_3) \\ b_d = \frac{1}{\sqrt{2}}(b_2 - b_3) \end{cases} \quad (6)$$

$$\begin{cases} a_c = \frac{1}{\sqrt{2}}(a_2 + a_3) \\ b_c = \frac{1}{\sqrt{2}}(b_2 + b_3) \end{cases} \quad (7)$$

From (6) and (7), the matrix \mathbf{S} of conventional scattering parameters in (3) can be converted into the matrix \mathbf{S}_{mix} of mix-mode ones as follows.

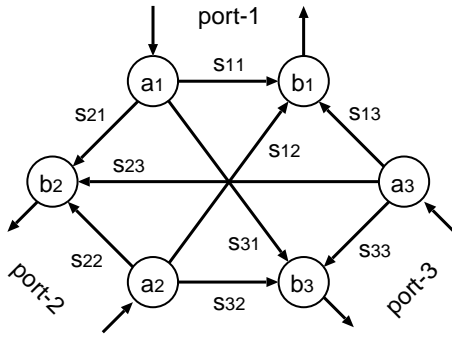


Figure 4: Network model of balanced SAW filter

$$\mathbf{S}_{mix} = \mathbf{T} \mathbf{S} \mathbf{T}^{-1} = \begin{bmatrix} s_{11} & s_{1d} & s_{1c} \\ s_{d1} & s_{dd} & s_{dc} \\ s_{c1} & s_{cd} & s_{cc} \end{bmatrix} \quad (8)$$

where, matrix \mathbf{T} is given as follows.

$$\mathbf{T} = \frac{1}{\sqrt{2}} \begin{bmatrix} \sqrt{2} & 0 & 0 \\ 0 & 1 & -1 \\ 0 & 1 & 1 \end{bmatrix}$$

By using the above mix-mode scattering parameters instead of conventional ones, we evaluate the band-pass filter characteristics of the balanced SAW filter in the same way with the unbalanced one[7]. Therefore, the standing wave ratios of the input-port E_3 and the output-port E_4 can be defined by (9) and (10). The attenuation E_5 between the input-port and the output-port is also defined as shown in (11).

$$E_3 = \frac{1 + |s_{11}|}{1 - |s_{11}|} \quad (9)$$

$$E_4 = \frac{1 + |s_{dd}|}{1 - |s_{dd}|} \quad (10)$$

$$E_5 = 20 \log_{10}(|s_{d1}|) \quad (11)$$

3 Problem Formulation

3.1 Design Parameters

In order to describe a suitable structure of the balanced SAW filter, we have to select appropriate design parameters such as the numbers of fingers for IDTs, the number of strips for SMSA, the width and the length of electrodes, and so on. Therefore, the design parameters of the balanced SAW filter usually take not only continuous values but also discrete values.

We represent the design parameters of the balanced SAW filter as $\mathbf{x} = (x_1, \dots, x_D)$. Besides,

we specify the upper x_j^U and the lower x_j^L bounds for each of the design parameters $x_j \in \mathbf{x}$ as follows.

$$x_j^L \leq x_j \leq x_j^U, \quad j = 1, \dots, D. \quad (12)$$

3.2 Optimum Design Problem

By using the criteria E_h ($h = 1, \dots, 5$) described in the previous section, we define M objective functions $f_m(\mathbf{x})$ ($m = 1, \dots, M$) and K constraints $g_k(\mathbf{x})$ ($k = 1, \dots, K$). Then we formulate the structural design of the balanced SAW filter as a constrained multi-objective optimization problem in (13).

$$\begin{cases} \text{minimize} & \{ f_1(\mathbf{x}), \dots, f_M(\mathbf{x}) \} \\ \text{subject to} & g_k(\mathbf{x}) \leq 0, \quad k = 1, \dots, K. \\ & x_j^L \leq x_j \leq x_j^U, \quad j = 1, \dots, D. \end{cases} \quad (13)$$

4 Differential Evolution (GDE3)

4.1 Overview of GDE3

Differential Evolution (DE)[13] is one of the most recent Evolutionary Algorithms (EAs) for solving real-parameter optimization problems. DE exhibits an overall excellent performance for a wide range of benchmark problems. Furthermore, because of its simple but powerful searching capability, DE has got numerous real-world applications[18]. Recently, due to this success, DE has been extended to other types of problems, such as multi-objective optimization[19].

Non-dominated Sorting Genetic Algorithm-II (NSGA-II)[20] proposed by Deb et al. is one of the most famous Evolutionary Multi-objective Optimization (EMO) algorithms. In order to obtain a set of various Pareto optimal solutions, the non-dominated sorting, ranking, and elitism techniques are utilized in the survival selection of NSGA-II. Therefore, some of the multi-objective DEs have combined the effective searching strategy of DE with the survival selection of NSGA-II. For example, Iorio and Li[21] have proposed Non-dominated Sorting DE (NSDE).

Generalized DE 3 (GDE3)[15] is an extended version of the basic DE for constrained multi-objective optimization. The selection mechanism in GDE3 considers Pareto dominance when comparing feasible solutions, and weak dominance when comparing infeasible solutions. Feasible solutions are always preferred over infeasible ones, regardless of Pareto dominance. Furthermore, the survival selection based on non-dominated sorting and crowding distance, which have been contrived originally for NSGA-II[20], are also adopted in GDE3. GDE3 is tested with a set of various types of benchmark problems and results show an improved diversity of the final solutions over

NSGA-II as well as demonstrating a reduction in the number of needed function evaluations[15].

4.2 Representation of Solution

GDE3 is usually used to solve the constrained multi-objective optimization problem over the D ($D \geq 1$) dimensional real-parameters. GDE3 holds N_P individuals, or the candidate solutions of the multi-objective optimization problem, in the population. As well as conventional real-coded GAs[22], every individual of GDE3 is coded as a D -dimensional real-parameter vector. Therefore, the i -th individual \mathbf{x}_i^G ($i = 1, \dots, N_P$) included in the population of the generation G ($G \geq 0$) is represented as follows.

$$\mathbf{x}_i^G = (x_{1,i}^G, \dots, x_{j,i}^G, \dots, x_{D,i}^G) \quad (14)$$

where, $0 \leq x_{j,i}^G \leq 1$ ($j = 1, \dots, D$).

Each design parameter $x_j \in \mathbf{x}$ used to describe the structure of the balanced SAW filter takes either a continuous value or a discrete value. Therefore, in order to apply GDE3 to the optimum design problem of the balanced SAW filter formulated in (13), we employ the following technique that converts an individual \mathbf{x}_i^G into the corresponding solution \mathbf{x} [12].

In the regularized continuous search space of GDE3, each element of the individual $x_{j,i}^G \in \mathbf{x}_i^G$ is restricted within the range between 0 and 1 as shown in (14). Therefore, each element $x_{j,i}^G \in \mathbf{x}_i^G$ is converted into the corresponding design parameter $x_j \in \mathbf{x}$ when the values of the objective functions $f_m(\mathbf{x})$ and/or the constraints $g_k(\mathbf{x})$ are evaluated. If a design parameter $x_j \in \mathbf{x}$ takes a continuous value originally, the corresponding $x_{j,i}^G \in \mathbf{x}_i^G$ is converted into the design parameter as shown in (15). On the other hand, if a design parameter $x_j \in \mathbf{x}$ takes a discrete value with an interval e_j , the corresponding $x_{j,i}^G \in \mathbf{x}_i^G$ is converted into the design parameter as shown in (16).

$$x_j = (x_j^U - x_j^L) x_{j,i}^G + x_j^L \quad (15)$$

$$x_j = \text{round} \left(\frac{(x_j^U - x_j^L) x_{j,i}^G}{e_j} \right) e_j + x_j^L \quad (16)$$

where, $\text{round}(z)$ rounds $z \in \mathbb{R}$ to the nearest integer.

4.3 Procedure of GDE3

In the beginning of the procedure of GDE3, a set of individuals \mathbf{x}_i^G ($i = 1, \dots, N_P$) are generated randomly as an initial population $\mathbf{x}_i^G \in \mathbf{P}^G$ ($G = 0$).

Then, in each generation G ($G = 0, \dots, G_{max}$), GDE3 goes through each individual $\mathbf{x}_i^G \in \mathbf{P}^G$, which is called the target vector, and generates trial vectors \mathbf{u}_i^G from \mathbf{x}_i^G with the genetic operator in (17). The

genetic operator in (17) is equivalent to the strategy of DE called " DE/rand/1/bin " [13]. Therefore, three individuals \mathbf{x}_{r1}^G , \mathbf{x}_{r2}^G and \mathbf{x}_{r3}^G ($r1 \neq r2 \neq r3 \neq i$) are selected randomly from the population \mathbf{P}^G .

$$\left[\begin{array}{l} j_{rand} = \text{rand}[1, D] \\ \text{for}(j = 1; j \leq D; j = j + 1)\{ \\ \quad \text{if}(\text{rand}[0, 1] < C_R \vee j = j_{rand})\{ \\ \quad \quad \mathbf{u}_{j,i}^G = \mathbf{x}_{j,r1}^G + S_F (\mathbf{x}_{j,r2}^G - \mathbf{x}_{j,r3}^G) \\ \quad \quad \} \text{else}\{ \\ \quad \quad \quad \mathbf{u}_{j,i}^G = \mathbf{x}_{j,i}^G \\ \quad \quad \quad \} \\ \quad \} \end{array} \right. \quad (17)$$

where, the subscript $j_r \in [1, D]$ is selected randomly. The scale factor $S_F \in (0, 1+]$ and the crossover rate $C_R \in [0, 1]$ are user-defined control parameters.

Before we describe the survival selection of GDE3, we will explain the dominance relationship between the trial vector \mathbf{u}_i^G and the target vector \mathbf{x}_i^G . Weak dominance relation between two vectors is defined such that \mathbf{u}_i^G weakly dominates \mathbf{x}_i^G iff $\forall m : f_m(\mathbf{u}_i^G) \leq f_m(\mathbf{x}_i^G)$. Dominance relation between two vectors is also defined such that \mathbf{u}_i^G dominates \mathbf{x}_i^G iff $\forall m : f_m(\mathbf{u}_i^G) < f_m(\mathbf{x}_i^G)$. The dominance relationship can be extended to take into consideration constraint values besides objective values[15].

Each trial vector \mathbf{u}_i^G ($i = 1, \dots, N_P$) is compared with the corresponding target vector \mathbf{x}_i^G . Then, according to the following rules, either the trial vector \mathbf{u}_i^G or the target vector \mathbf{x}_i^G is selected as the member of the next population \mathbf{P}^{G+1} for the time being[15].

- o If both vectors are infeasible, then the trial vector \mathbf{u}_i^G is selected if it weakly dominates \mathbf{x}_i^G in the constraint violation space. Otherwise \mathbf{x}_i^G is selected.
- o If one vector is feasible and the other is infeasible, then the feasible vector is selected.
- o In the case that both vectors are feasible, then the trial vector \mathbf{u}_i^G is selected if it weakly dominates \mathbf{x}_i^G in the objective function space. On the other hand, if \mathbf{x}_i^G dominates \mathbf{u}_i^G , then \mathbf{x}_i^G is selected. If neither vector dominates each other in the objective function space, then both vectors are selected.

After the above selection in each generation, the size of the next population \mathbf{P}^{G+1} may have increased over the original size N_P . If that is the case, the size of the population \mathbf{P}^{G+1} is decreased back to the original size based on a similar selection approach used in NSGA-II[20]. Exactly speaking, the individuals of the population \mathbf{P}^{G+1} are sorted based on non-dominance and crowdedness. Then the inferior individuals according to these measurements are removed from \mathbf{P}^{G+1} to decrease the size of \mathbf{P}^{G+1} to N_P .

Table 1: Design parameters of balanced SAW filter

x_j	$[x_j^L, x_j^U]$	e_j	design parameter
x_1	[200, 400]	–	overlap between electrodes
x_2	[10.0, 40.0]	0.5	number of fingers of IDT-R
x_3	[10.5, 40.5]	1.0	ditto of IDT-T
x_4	[1.0, 4.0]	1.0	ditto of modulated IDT
x_5	[50.0, 300.0]	10.0	number of strips of SMSA
x_6	[0.2, 0.8]	–	metallization ratio of IDT
x_7	[0.2, 0.8]	–	ditto of SMSA
x_8	[1.0, 1.1]	–	pitch ratio of SMSA
x_9	[0.9, 1.0]	–	ditto of modulated IDT
x_{10}	[1.9, 2.1]	–	finger pitch of IDT
x_{11}	[3900, 4000]	–	thickness of electrode

5 Three-objective Design Problem

5.1 Design Parameters

In order to describe the structure of the balanced SAW filter in Fig. 1, we have selected $D = 11$ design parameters $x_j \in \mathbf{x}$ ($j = 1, \dots, D$) as shown in Table 1. Besides the design parameters $x_j \in \mathbf{x}$, Table 1 shows their upper x_j^U and lower x_j^L bounds. Furthermore, the intervals $e_j \in \mathbb{R}$ of design parameters $x_j \in \mathbf{x}$ are also described in Table 1 if corresponding design parameters x_j have to take discrete values.

5.2 Objectives and Constraints

We formulate the structural design of the balanced SAW filter shown in Fig. 1 as a three-objective optimization problem with six non-linear constraints.

First of all, the values of the criteria E_h for the balanced SAW filter depend on both the frequency ω and the design parameters \mathbf{x} . Therefore, we choose a set of sample points $\omega \in \Omega_P$ from the pass-band of the balanced SAW filter. Similarly, we choose two sets of sample points $\omega \in \Omega_L$ and $\omega \in \Omega_H$ respectively from the lower and the higher stop-bands.

Because the balanced SAW filter works as a band-pass filter, by using the attenuation $E_5 = E_5(\mathbf{x}, \omega)$ in (11), we define the following three objective functions $f_m(\mathbf{x})$ ($m = 1, 2, 3$) to be minimized. The attenuation of the balanced SAW to be optimized by using three objective functions is illustrated in Fig. 5.

$$f_1(\mathbf{x}) = \sum_{\omega \in \Omega_L} \frac{E_5(\mathbf{x}, \omega)}{|\Omega_L|} \quad (18)$$

$$f_2(\mathbf{x}) = \sum_{\omega \in \Omega_H} \frac{E_5(\mathbf{x}, \omega)}{|\Omega_H|} \quad (19)$$

$$f_3(\mathbf{x}) = - \left(\sum_{\omega \in \Omega_P} \frac{E_5(\mathbf{x}, \omega)}{|\Omega_P|} \right) \quad (20)$$

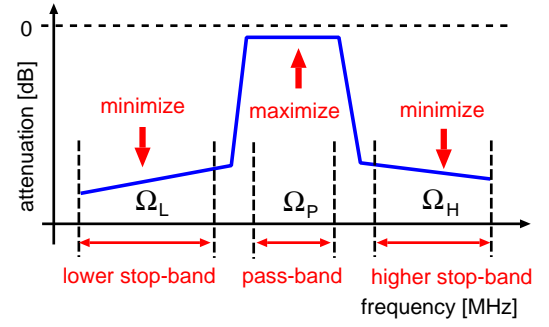


Figure 5: Three objectives for attenuation

We specify the upper $U_h(\omega)$ and the lower $L_h(\omega)$ bounds for the other criteria $E_h(\omega, \mathbf{x})$. Then the four of the six constraints $g_k(\mathbf{x}) \leq 0$ ($k = 1, \dots, 4$) are given as shown in (21). The rest two constraints are given respectively as shown in (22) and (23).

$$g_k(\mathbf{x}) = \sum_{\omega \in \Omega_P} \frac{E_k(\mathbf{x}, \omega) - U_k(\omega)}{|\Omega_P|} \leq 0 \quad (21)$$

$$g_5(\mathbf{x}) = \sum_{\omega \in \Omega_P} \frac{L_1(\omega) - E_1(\mathbf{x}, \omega)}{|\Omega_P|} \leq 0 \quad (22)$$

$$g_6(\mathbf{x}) = \sum_{\omega \in \Omega_P} \frac{L_2(\omega) - E_2(\mathbf{x}, \omega)}{|\Omega_P|} \leq 0 \quad (23)$$

5.3 Optimum Design Problem

From (18) ~ (23), we formulate the structural design of the balanced SAW filter as a constrained multi-objective optimization problem shown in (24).

$$\begin{cases} \text{minimize} & \{f_1(\mathbf{x}), f_2(\mathbf{x}), f_3(\mathbf{x})\} \\ \text{subject to} & g_k(\mathbf{x}) \leq 0, k = 1, \dots, 6. \\ & x_j^L \leq x_j \leq x_j^U, j = 1, \dots, D. \end{cases} \quad (24)$$

The objective functions $f_m(\mathbf{x})$ and the constraints $g_k(\mathbf{x})$ shown in (24) are evaluated at 401 sample points $\omega \in \Omega_L \cup \Omega_P \cup \Omega_H$ within the range between 850[MHz] and 1080[MHz]. The pass-band is selected to the range between 950[MHz] and 980[MHz].

5.4 Experiment and Result

We applied GDE3 to the three-objective optimization problem in (24). As the stopping condition of GDE3, the maximum generation was limited to $G_{max} = 800$. The control parameters of GDE3 were given as follows: the population size $N_P = 200$, the scale factor $S_F = 0.9$ and the crossover rate $C_R = 0.9$. These values were decided considering the result of the empirical study about the control parameters of GDE3[23].

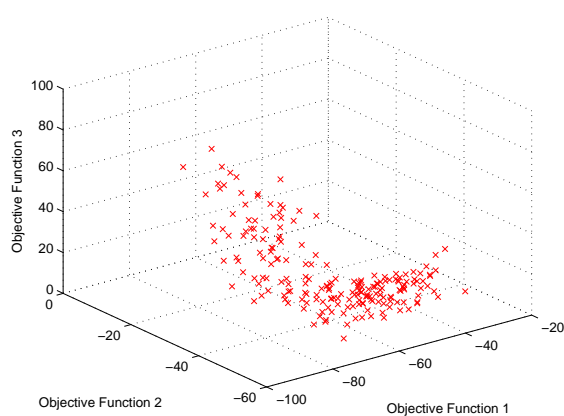
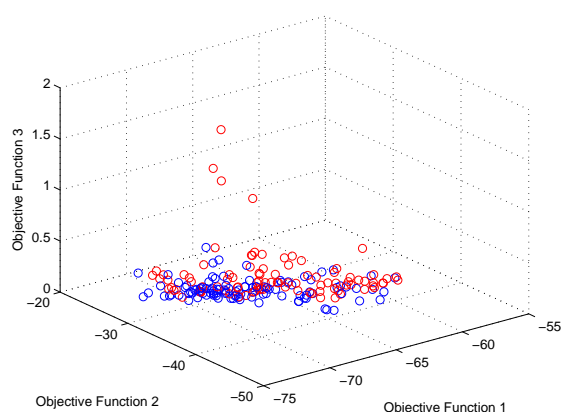
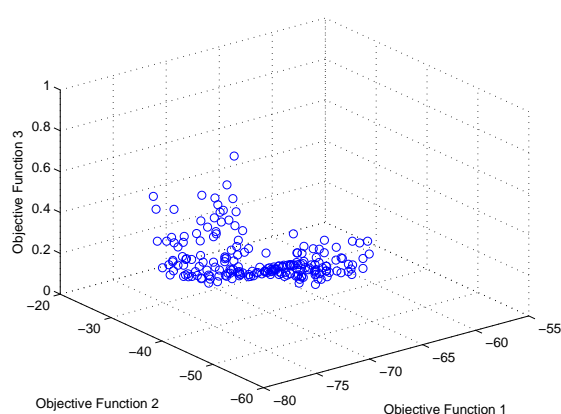
(a) generation: $G = 0$ (b) generation: $G = 200$ (c) generation: $G = 800$ Figure 6: Progress of the population in three-objective function space (population size: $N_P = 200$)

Table 2: Result of PCA

	ζ_1	ζ_2	ζ_3
f_1	-0.615	-0.524	+0.588
f_2	-0.229	-0.833	+0.502
f_3	+0.754	-0.174	+0.633
α_m	0.506	0.918	1.00

Incidentally, the program of GDE3 including the simulator for the balanced SAW filter shown in Fig. 1 is coded by MATLAB. The program spends about one hour for one run on a PC (CPU: Intel(R) Core 2).

Figure 6 depicts all individuals of the populations of different generations in the objective function space. In Fig. 6, infeasible individuals are denoted by cross symbol (\times), while feasible ones are denoted by circle symbol (\circ). Furthermore, non-dominated feasible individuals are denoted by blue circle, while dominated feasible ones are denoted by red circle.

Comparing three populations achieved at respective generations, we can see that the great progress of the multi-objective search has been made by GDE3. First of all, randomly generated individuals of the initial population ($G = 0$) are worse and infeasible. However, the objective function values of all individuals are improved and a lot of feasible individuals are found after $G = 200$ generations. Finally, at the maximum generation $G_{max} = 800$, all individuals become feasible and they are non-dominated each other.

5.5 Analysis and Discussion

As you can see in Fig. 6, it is difficult to understand the relationship among objectives graphically if there are more than three objectives. Therefore, Principal Component Analysis (PCA) has been used successfully to assess a set of the Pareto-optimal solutions obtained by EMO algorithms[24, 25]. In order to clarify the tradeoff relationship among the three objectives in Fig. 6 (c), we have also applied PCA to the set of the non-dominated solutions obtained by GDE3.

Table 2 shows the result of PCA in which eigenvectors ζ_m ($m = 1, 2, 3$) and accumulated proportions α_m are listed. Because $\alpha_2 > 90\%$ holds in Table 2, we may pay attention only to the first and the second principal components. Furthermore, considering the objective functions corresponding to the most positive and the most negative element of the first principal component ζ_1 , we can say that $f_1(\mathbf{x})$ and $f_3(\mathbf{x})$ are the two most critically conflicting objectives. Besides, $f_2(\mathbf{x})$ seems to be redundant for the three-objective optimization problem in (24).

6 Two-objective Design Problem

6.1 Objectives and Constraints

From the result of PCA about the three-objective optimization problem in (24), we could find that the attenuation $E_5(\mathbf{x}, \omega)$ within the higher stop-band ($\omega \in \Omega_H$) should not be selected as the objective function. Therefore, we will move it from the objective to the constraint by specifying its upper bound $U_5(\omega)$ ($\omega \in \Omega_H$). Then we formulate the structural design of the balanced SAW filter shown in Fig. 1 as a constrained two-objective optimization problem.

First of all, we consider the same design parameters with those of the three-objective optimization problem shown in Table 1. By using the attenuation $E_5(\mathbf{x}, \omega)$, we define the following two objective functions $\hat{f}_m(\mathbf{x})$ ($m = 1, 2$) to be minimized. The attenuation of the balanced SAW filter compelled by two objectives and one constraint is shown in Fig. 7.

$$\hat{f}_1(\mathbf{x}) = - \left(\sum_{\omega \in \Omega_P} \frac{E_5(\mathbf{x}, \omega)}{|\Omega_P|} \right) \quad (25)$$

$$\hat{f}_2(\mathbf{x}) = \sum_{\omega \in \Omega_L} \frac{E_5(\mathbf{x}, \omega)}{|\Omega_L|} \quad (26)$$

We specify the upper $U_h(\omega)$ and the lower $L_h(\omega)$ bounds for the other criteria $E_h(\omega, \mathbf{x})$. Then the four of the seven constraints $g_k(\mathbf{x}) \leq 0$ ($k = 1, \dots, 4$) are given by (27). The rest three constraints are given respectively as shown in (28), (29) and (30).

$$g_k(\mathbf{x}) = \sum_{\omega \in \Omega_P} \frac{E_k(\mathbf{x}, \omega) - U_k(\omega)}{|\Omega_P|} \leq 0 \quad (27)$$

$$g_5(\mathbf{x}) = \sum_{\omega \in \Omega_P} \frac{L_1(\omega) - E_1(\mathbf{x}, \omega)}{|\Omega_P|} \leq 0 \quad (28)$$

$$g_6(\mathbf{x}) = \sum_{\omega \in \Omega_P} \frac{L_2(\omega) - E_2(\mathbf{x}, \omega)}{|\Omega_P|} \leq 0 \quad (29)$$

$$g_7(\mathbf{x}) = \sum_{\omega \in \Omega_H} \frac{E_5(\mathbf{x}, \omega) - U_5(\omega)}{|\Omega_H|} \leq 0 \quad (30)$$

6.2 Optimum Design Problem

From (25) ~ (30), we formulate the structural design of the balanced SAW filter as a constrained two-objective optimization problem shown in (31).

$$\left[\begin{array}{l} \text{minimize} \quad \{ \hat{f}_1(\mathbf{x}), \hat{f}_2(\mathbf{x}) \} \\ \text{subject to} \quad g_k(\mathbf{x}) \leq 0, \quad k = 1, \dots, 7. \\ \quad \quad \quad x_j^L \leq x_j \leq x_j^U, \quad j = 1, \dots, D. \end{array} \right. \quad (31)$$

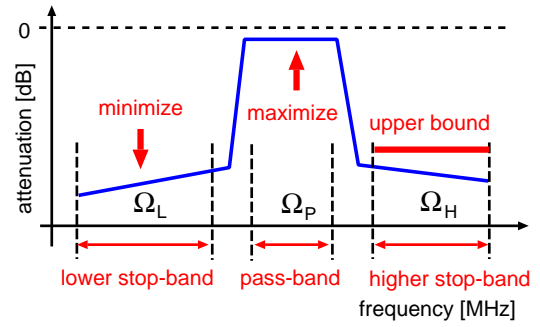


Figure 7: Two objectives for attenuation

6.3 Experiment and Result

We applied GDE3 to the two-objective optimization problem in (31). As the stopping condition of GDE3, the maximum generation was limited to $G_{max} = 500$. The control parameters of GDE3 were given as follows: the population size $N_P = 100$, the scale factor $S_F = 0.9$ and the crossover rate $C_R = 0.9$.

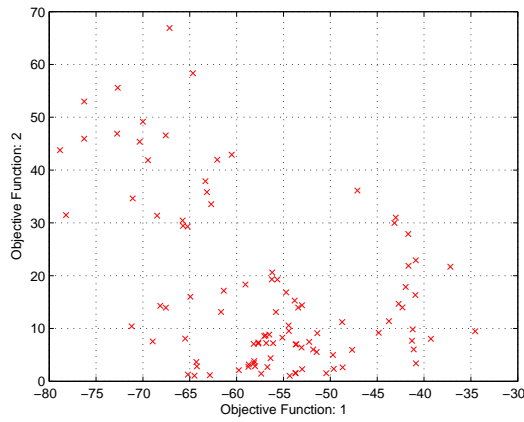
Figure 8 depicts all individuals of the populations of different generations in the same way with Fig. 6. Comparing the populations achieved at respective generations, we can observe the great progress of the multi-objective search. Besides, we can clearly confirm the tradeoff relationship between two objectives at the maximum generation ($G_{max} = 500$).

Applying GDE3 to the two-objective optimization problem in (31), we could obtain 26 non-dominated feasible solutions denoted by blue circle in Fig. 8 (c). In order to verify the qualities of these final solutions, we have taken two samples from them. Figure 9 shows the attenuations $E_5(\mathbf{x}, \omega)$ and the objective values ($\hat{f}_1(\mathbf{x}), \hat{f}_2(\mathbf{x})$) of the two solutions.

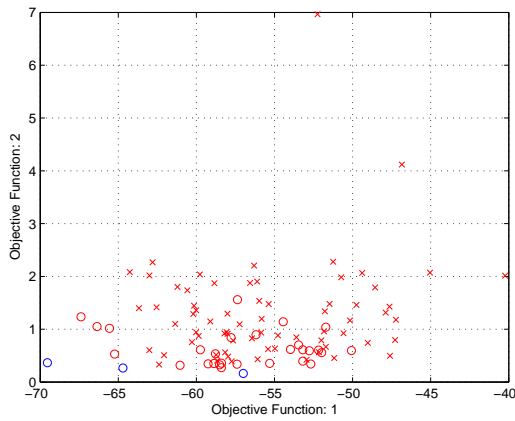
7 Conclusion

A multi-objective optimum design method for balanced SAW filters was proposed. First of all, the structural design of the balanced SAW filter was formulated as a constrained three-objective optimization problem. Then GED3 was applied to the optimization problem. In order to assess the set of the non-dominated solutions obtained by GDE3, PCA was employed. As a result, we could find that the two of the three objective functions were clearly conflicting but one of them is redundant. Therefore, two-objective optimization problem was formulated and GDE3 was applied to the optimization problem again.

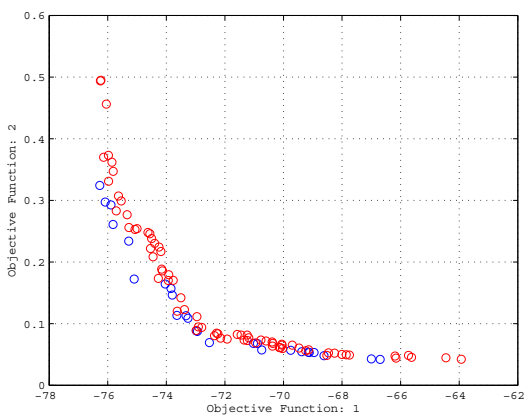
Future work will focus on the further investigation of the set of the Pareto-optimal solutions in the design parameter space. Thereby we would like to clarify the relationship between the structure and the frequency response of the balanced SAW filter.



(a) generation: $G = 0$

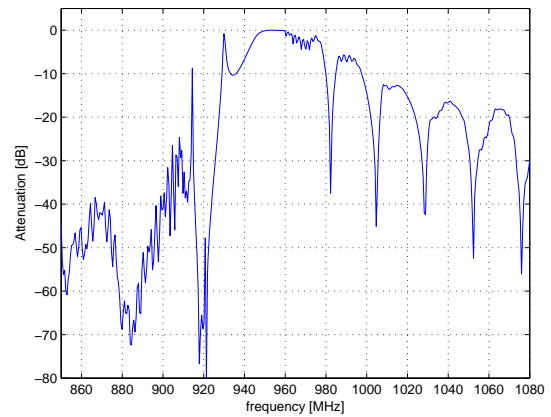


(b) generation: $G = 50$

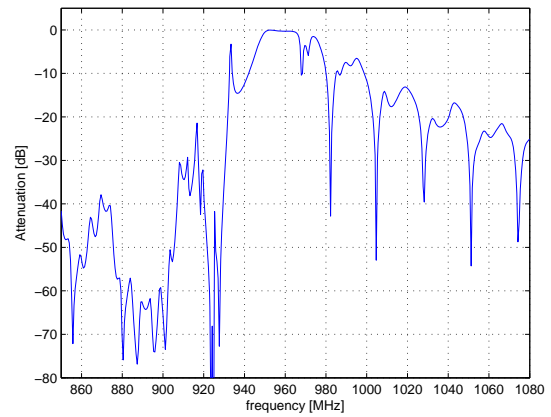


(c) generation: $G = 500$

Figure 8: Progress of the population in two-objective function space (population size: $N_P = 100$)



$$(\hat{f}_1(\mathbf{x}), \hat{f}_2(\mathbf{x})) = (-67.003, 0.042)$$



$$(\hat{f}_1(\mathbf{x}), \hat{f}_2(\mathbf{x})) = (-76.273, 0.324)$$

Figure 9: Attenuations of final solutions

Acknowledgements: The research was supported in part by the Grant-in-Aid for Scientific Research (C) (Project No. 21560432) from Japan Society for the Promotion of Science (JSPS).

References:

- [1] C. K. Campbell: *Surface Acoustic Wave Devices for Mobile and Wireless Communication*, Academic Press, 1998.
- [2] K. Hashimoto: *Surface Acoustic Wave Devices in Telecommunications – Modeling and Simulation*, Springer, 2000.
- [3] H. Meier, T. Baier and G. Riha: Miniaturization and advanced functionalities of SAW devices. *IEEE Trans. on Microwave Theory and Techniques*, Vol. 49, No. 2, 2001, pp. 743–748.
- [4] M. Koshino, H. Kanasaki, T. Yamashita, S. Mitobe, Y. Kawase, Y. Kuroda and Y. Ebata: Sim-

- ulation modeling and correction method for balance performance of RF SAW filters, *Proceedings of IEEE Ultrasonics Symposium*, 2002, pp. 301–305.
- [5] S. Goto and T. Kawakatsu: Optimization of the SAW filter design by immune algorithm, *Proceedings of IEEE International Ultrasonics Ferroelectrics, and Frequency Control Joint 50th Anniversary Conference*, 2004, pp. 600–603.
- [6] N. Khalil, A. Zaki, M. B. Salen and H. Ali: Optimum design of MEMS-SAW filter for wireless system applications, *Proceedings of the 5th WSEAS International Conference on Circuits, Systems, Electronics, Control and Signal Processing*, 2006.
- [7] K. Tagawa and H. Kim: A local search technique for large-scale optimum design problems of double mode SAW filters, *WSEAS Trans. on Circuits and Systems*, Issue 1, Vol. 6, 2007, pp. 1–8.
- [8] L-Y. Chang and H-C. Chen: Tuning of fractional PID controllers using adaptive genetic algorithm for active magnetic bearing system, *WSEAS Trans. on Systems*, Issue 1, Vol. 8, 2009, pp. 158–167.
- [9] D. Vućina, Ž. Lozina and I. Pehnc: Coupled evolutionary shape optimization and reverse engineering in product design and virtual prototyping, *WSEAS Trans. on Systems*, Issue 3, Vol. 8, 2009, pp. 390–399.
- [10] K. Tagawa, T. Yamamoto, T. Igaki and S. Seki: An Imanishian genetic algorithm for the optimum design of surface acoustic wave filter, *Proceedings of the 2003 IEEE Congress on Evolutionary Computation*, pp. 2748–2755, 2003.
- [11] J. Meltaus, P. Hamalainen, M. Salomaa and V. P. Plessky: Genetic optimization algorithms in the design of coupled SAW filters, *Proceedings of IEEE International Ultrasonics Ferroelectrics, and Frequency Control Joint 50th Anniversary Conference*, 2004, pp. 1901–1904.
- [12] K. Tagawa: Simulation modeling and optimization technique for balanced surface acoustic wave filters, *Proceedings of the 7th WSEAS International Conference on Simulation, Modelling and Optimization*, 2007, pp. 295–300.
- [13] R. Storn and K. Price: Differential evolution – a simple and efficient heuristic for global optimization over continuous space, *Journal of Global Optimization*, Vol. 11, No. 4, 1997, pp. 341–359.
- [14] T. Kojima and T. Suzuki, Fundamental equations of electro-acoustic conversion for an interdigital surface-acoustic-wave transducer by using force factors, *Japanese Journal of Applied Physics Supplement*, 31, 1992, pp. 194–197.
- [15] S. Kukkonen and J. Lampinen: GDE3: The third evolution step of generalized differential evolution, *Proceedings of the 2005 IEEE Congress on Evolutionary Computation*, 2005, pp. 443–450.
- [16] O. Kawachi, S. Mitobe, M. Tajima, T. Yamaji, S. Inoue and K. Hashimoto: A low-pass and wide-band DMS filter using pitch-modulated IDT and reflector structures, *Proceedings of IEEE International Ultrasonics Ferroelectrics, and Frequency Control Joint 50th Anniversary Conference*, 2004, pp. 298–301.
- [17] D. E. Bockelman and W. R. Eisenstadt: Combined differential and common-mode scattering parameters: theory and simulation, *IEEE Trans. on Microwave Theory and Techniques*, Vol. 43, No. 7, 1995, pp. 1530–1539.
- [18] K. V. Price, R. M. Storn and J. A. Lampinen: *Differential Evolution - A Practical Approach to Global Optimization*, Springer, 2005.
- [19] E. Mezura-Montes, M. Reyes-Sierra and C. A. Coello Coello: Multi-objective optimization using differential evolution: a survey of the state-of-art, *Advances in Differential Evolution*, Springer, 2008, pp. 173–196.
- [20] K. Deb, A. Pratap, S. Agarwal and T. Meyarivan: A fast and elitist multiobjective genetic algorithm: NSGA-II, *IEEE Trans. on Evolutionary Computation*, Vol. 6, No. 2, 2002, pp. 182–197.
- [21] A. W. Iorio and X. Li: Solving rotated multi-objective optimization problems using differential evolution, *AI2004: Advances in Artificial Intelligence, Lecture Notes in Computer Science*, Vol. 3339, 2004, pp. 861–872.
- [22] L. J. Eshelman and J. D. Schaffer: Real-coded genetic algorithms and interval-schemata, *Foundations Genetic Algorithms 2*, Morgan Kaufmann Publisher, 1993, pp. 187–202.
- [23] S. Kukkonen and J. Lampinen: A empirical study of control parameters for the third version of generalized differential evolution (GDE3), *Proceedings of the 2006 IEEE Congress on Evolutionary Computation*, 2006, pp. 7355–7362.
- [24] K. Deb and D. K. Saxena: Searching for Pareto-optimal solutions through dimensionality reduction for certain large-dimensional multi-objective optimization problem, *Proceedings of the 2006 IEEE Congress on Evolutionary Computation*, 2006, pp. 3353–3360.
- [25] L. Costa and P. Oliveira: Multiobjective optimization: redundant and informative objectives, *Proceedings of the 2009 IEEE Congress on Evolutionary Computation*, pp. 2008–2015, 2009.